International Journal of Thin Films Science and Technology

http://dx.doi.org/10.18576/ijtfst/130304

Banana Stem Extract was Used in the Green Production and Characterization of Silver Nanoparticles to Determine their Effectiveness as a Possible Anticancer Drug

*A. Sudha, R. Pradheepa and I. Manimehan**

Department of Physics, M.R. Government Arts College, Mannargudi (Affiliated to Bharathidasan University, Tiruchirappalli), Tamil Nadu, India

Received: 12 May 2024, Revised: 12 Jun. 2024, Accepted: 31 Jul. 2024
Published online: 1 Sep. 2024

Abstract: In this article, discussed about many potential use and applications in the biomedical sciences, bio-synthesized silver nanoparticles are a fascinating area of interest in the nanobiosciences. Even if several biological components are used in the green synthesis of silver nanoparticles, there is still a great deal of room for advancement in the production of stable and widely useful silver nanoparticles. Despite the various biological uses, silver nanoparticles mostly produced through biological means which have been evaluated as an antibacterial agent. Therefore, the objective of the current work is to highlight the use of biologically produced silver nanoparticles as anti-inflammatory agents. This study is also likely the first to assess the potential of banana stem extract to decrease AgNO3 to Ag-nanoparticles. UV-Vis spectroscopy, DLS, XRD, and zeta potential measurements were used to characterize the nanoparticles, and SEM and TEM were used to examine their morphology. The cytotoxicity of the synthesized nanoparticles and the anti-cancer effects of BSE via inducing apoptosis and its molecular indicators were assessed. This suggests that it could be a cutting-edge, environmentally acceptable method for producing non-toxic, cost-effective silver nanoparticles through biosynthesis.

Keywords: Green Synthesis, Banana, Cytotoxicity, Apoptosis, Cancer.

1 Introduction

The sole goal of raising humankind's living standards, researchers have been placed a strong emphasis on the topic of nanotechnology. In short, nanotechnology is a branch of engineering and science that deals with materials whose any one of their dimensions is within the nanoscale (about 1-100 nm) (Bayda S et al., 2019). It deals with proportions and tolerances of particles less than 100 nanometer (Murthy SK, 2007). Since the advent of science and technology, the synthesis of metal nanoparticles and nanocomposites has gained attention as a new topic for investigation and research in the field of material science because of their distinctive size and shape and other distinguishing characteristics from conventional bulk structures1, 2 (Jeevanandam et al., 2018). Metal nanoparticles have been widely utilised since the creation of nanomaterials (Yaqoob AA et al., 2020). Silver nanoparticles (AgNPs) have been widely used for the last several decades due to their unique properties and wide variety of applications. Silver nanoparticles (AgNPs) have become one of the most promising nanomaterials in recent years because of their distinctive characteristics, including Surface Enhanced Raman Scattering (SERS), improved electrical and thermal conductivity, and, most importantly, a variety of intriguing bioactivities12–16. Antifungal17, antioxidant18, antibacterial19, anti-inflammatory20, anticancer effects, and nonviral carrier in gene therapy are a few of these various bioactivities. Because they address the issue of bacterial drug resistance, AgNPs' antibacterial properties have received a lot of attention among other applications (Xu, et al., 2020). AgNPs can be produced via a wide range of techniques, including both physical and chemical ones22. Even if chemical methods are successful, because of the chemicals used and the difficulty in getting rid of them, these methods may be harmful (Beyene, et al., 2017). Environmental impact is also caused by the chemical chemicals utilised in these techniques23. In order to solve these issues, scientists are now concentrating on simple, environmentally friendly methods of producing metal nanoparticles24. These synthesis techniques provide an affordable, simple, and environmentally responsible option to create tailored metal nanoparticles (Bhardwaj, et al., 2020).

During the synthesis of nanoparticles, the stability of the particles plays a vital role, and in the majority of circumstances, it becomes challenging to obtain stable nanoparticles26. However, upon examination, the biosynthesized nanoparticles were fairly stable for around six weeks (Iravani, et al., 2014). The resulting AgNPs may be produced in enormous amounts and with very little expense. AgNPs were observed to range in size from 55 to 125 nm. The generated AgNPs have outstanding anti-inflammatory and good antibacterial effects (Naganthran, et al., 2022). An alternate material for antibacterial and anti-

*Corresponding author E-mail: manimehan@mrgac.ac.in

inflammatory drugs is provided by this hybrid nanomaterial (Hemeg, 2017).

After a thorough review of the literature, it was discovered that there hasn't been much done to assess the nano-precipitating ability of any mother tinctures, including the one made from banana stem extract for the preparation of silver nanoparticles, nor have there been many reports on the assessment of the biological activities of the AgNPs produced using mother tinctures, including those made from banana stem extract (Bhattacharyya, et al., 2012).

2 Materials and Methods

Merck India Pvt Ltd was used to buy silver nitrate. Dr. Willmar Schwabe India Pvt. Ltd. supplied the belladonna mother tincture. Diclofenac sodium from Novartis India Ltd. From Abbott, streptomycin was purchased. From Gibco,MTT, we acquired RPMI-1640, FBS was purchased from Thermo Fisher Scientific, and Himedia provided the penicillin-streptomycin solution.

2.1. Silver nanoparticle synthesis:

The final concentrations are 1mM, 2.5mM, 5mM, and 10mM after different concentrations of 20mM silver nitrate solution in Double Distilled water (D.D) water were mixed with 10x diluted belladonna mother tincture. For two hours, the reaction mixture was constantly stirred at 80 °C and 800 rpm. Due to the creation of silver nanoparticles, the solution's colour altered from pale yellow to red wine (Korbekandi, et al., 2014).

2.2. Characterization:

In the UV-VIS spectroscopy, the nanoparticles were scanned from 300 to 800 nm (Carry 60).

Polydispersity indices (PDIs) and average hydrodynamic diameters were measured using dynamic light scattering (DLS) (Ahsan, et al., 2020). (Malvern Instruments, UK; Malvern Zetasizer Nano-ZS). Each sample was examined three times at a temperature of 20 °C and a scattering angle of 173 °. The reference-dispersing medium was pure Double Distilled (D.D.) water (Stetefeld, et al., 2016).

The zeta potential of the sample (Malvern Zetasizer Nano-ZS, Malvern Instruments, UK) in D.D. water was also determined by electrophoretic light scattering at 25 °C, 150 V, in triplicate.

A Panalytical, X'Pertat 40 kV and 30 mA at a 2-angle pattern X-ray diffraction (XRD) study was performed to examine the crystalline phases of the silver nanoparticle sample. Between 20° and 80° was the range covered by the scanning (Arokiyaraj, et al., 2014).

To determine the functional groups that cap the synthesized silver nanoparticles, FTIR analysis was used to scan the particles. The KBr pellet (FTIR grade) method was used to conduct the analysis, and the spectrum was recorded using an FTIR device made by Bruker in the USA (alpha model).

SEM with the Inspect F50 SEM is used to observe the nanoparticles' morphology. The samples (surface or cross-sections) were cast on a tiny glass slide for imaging, and after mounting on double-sided carbon tape, were coated with a thin layer of palladium gold alloy.

The silver nanoparticles' morphology, size, and shape were assessed by TEM. JEM-2100 performed the TEM measurements. A drop of the diluted solution was applied to a copper grid that had been coated with carbon before being allowed to dry for 48 hours to prepare the TEM grid (Jagtap, et al., 2022).

The JEOL 2100 UHR-TEM instrument's EDAX detector was used to perform the EDAX study of the silver nanoparticles.

2.3. Cytotoxicity assay

A straightforward, non-radioactive calorimetric technique called MTT [3-(4,5-dimethylthazol-2-yl)-2-5-diphenyl tetrazolium bromide] is used to evaluate cell cytotoxicity in vitro (Sharma, et al., 2008). In 96 well plates, HeLa cells (1 106 cells/ml) were put before being incubated at 37 °C. After undergoing an overnight growth phase, cells were exposed to varying concentrations of free BSE and BSENPs. Untreated cells served as the control, and the cells were then incubated for 24 hours at 37°C in a humidified atmosphere of 5% CO2 and 95% oxygen. The cells were already incubated when MTT solutions were introduced, after which the media was removed after another 4 hours of incubation. After removing the supernatant from the cells after a 10-minute centrifugation, 200 mL of DMSO was added to each tube containing the cells. At 540 nm, the absorbance was measured with a microplate reader (Buranaamnuay, 2021).

2.4. Using the acridine orange-ethidium bromide dual staining approach, apoptosis-related morphological alterations

Condensed chromatin of dead apoptotic cells could be seen thanks to DNA staining with AO and EtBr. Since AO is cell permeable, it stains every cell, whether it is living or dead. DNA is compressed and broken apart during apoptosis. This can be seen when there are multiple tiny DNA patches in the cells. Later, dyes like EtBr can pass through the cell membrane. The intercalation of EtBr with DNA causes the DNA spots to become orange-red (Sigmon and Larcom, 1996). The cells were stained with AO/EtBr in a 1:1 ratio after being incubated with NARNPs for 24 hours. After two PBS washes, stained cells were examined under a fluorescence microscope. A function of the overall number of cells in the field was used to count the number of cells exhibiting apoptotic characteristics (Sathishkumar, et al., 2009).

2.5 Analysis of apoptosis using the ELIZA method

Statistic evaluation

The statistical program of social science (SPSS) version 11.0 for Windows was used to conduct the one-way analysis of

variance (ANOVA) and Duncan's multiple range test (DMRT). S.D. values are given for each group's six samples. P values less than 0.05 were regarded as significant (Salgame, et al., 1997).

3 Results and Discussion

3.1. Synthesis of silver nanoparticles

Several phytochemicals, including alkaloids such atropine, apoatropine, hysocyamine, and belladonine, are known to be present in banana stem extract (Soni, et al., 2012). These alkaloids are responsible for the suggested mechanism for the creation of silver nanoparticles. Alkaloids' surfaces attract silver ions, which are then reduced by other phytochemicals and result in the formation of silver nuclei. These newly created silver nuclei gather together and enlarge over time, eventually forming the silver nanoparticle (Zeng, et al., 2021).

The silver nanoparticles in this work create a self-assembled chain line structure since this reaction takes longer than the typical and ordinary synthesis of silver nanoparticles. Alkaloids in the extract formulation further cap the silver nanoparticles to prevent them from aggregating, which may also be the cause of the creation of a stable chain-like structure (Iravanil, et al., 2014).

3.2. Description of artificial silver nanoparticles

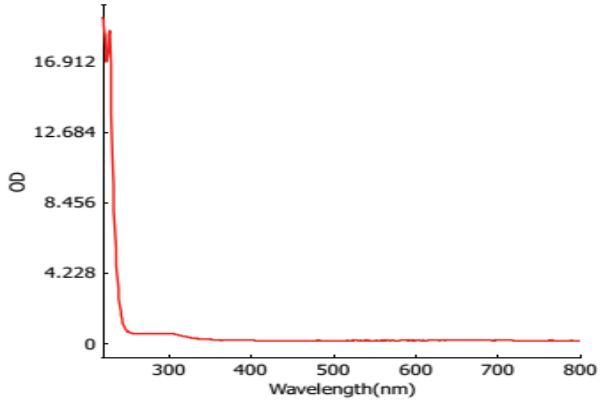

Fig. 1: UV-vis spectra of biologically produced AgNPs at various AgNO3 concentrations

The production of silver nanoparticles was indicated by an absorption band in the UV-visible spectrum at about 428 nm39. After 2 hours of reaction time, the peak was noticed. Figure 1 shows the UV-Visible spectrum of silver nanoparticles produced using banana stem extract. The 5mM sample was chosen for the upcoming work from the UV-VIS investigation because it had the highest peak among the four generated samples (Naganthran, et al., 2022).

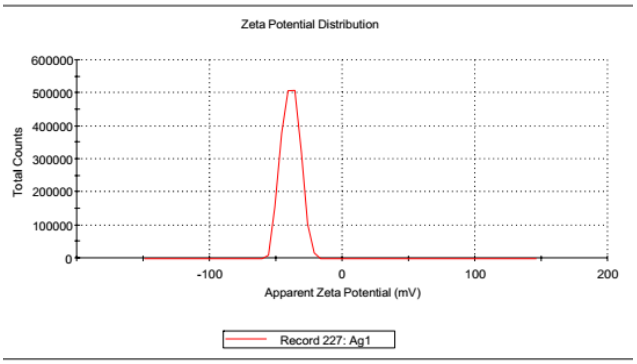

Fig. 2: Zeta potential of biomade silver nanoparticles

The particles' surface potential was highly negative, as shown by their Zeta potential, which was measured to be -31.3 0.786 mV. The nanoparticles' high negative Zeta Potential demonstrates their extreme stability. After a month, the hydrodynamic size was tested to validate stability, and the findings revealed little change in size from the first day of synthesis, as seen in Figure 2. After 30 days, the average size was 31.32 4.32 nm, despite some changes in the distribution pattern. 9. Figure 2 shows the size distribution of nanoparticles and the zeta potential (Erdogan, et al., 2019).

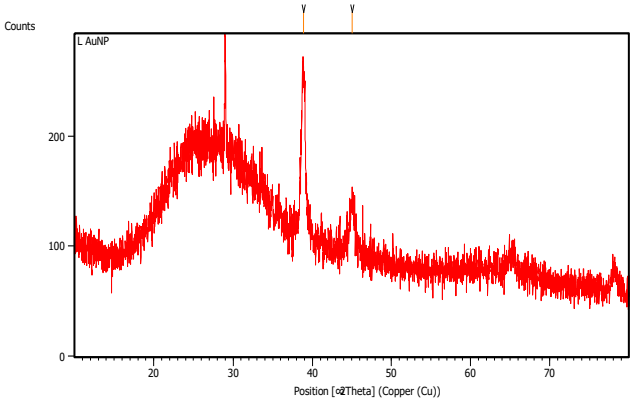

Fig. 3: The biosynthesized silver nanoparticles underwent XRD analysis

Table 1:

Pos. [°2Th.]	Height [cts]	FWHM Left [°2Th.]	d-spacing [Å]	Rel. Int. [%]
38.9011	**144.71**	**0.4684**	**2.31513**	**100.00**
45.0776	**46.66**	**0.5353**	**2.01127**	**32.25**

The biosynthesized silver nanoparticles were exposed to powder XRD in order to determine the structural information and validate the presence of silver nanoparticles. The XRD pattern of the created silver nanoparticles is displayed in Figure 3.

The pattern shows 2 significant peaks at (2) 38.901 and 45.0776, respectively, which correspond to the (144.71) and (46.66) planes. In addition to this, a sharp peak at 32.36 was

seen, which was associated with the plane 101 as previously reported40. The silver nanoparticles' FCC structure is consistent with the peak orientation. The Debye-Scherer equation was used to compute the crystalline size of silver nanoparticles41: These peaks may have arisen because the silver nanoparticles' surface is covered in a variety of organic and phytochemical substances. The table that is attached to Figure provides specific information on crystal size and lattice strain (David and Moldovan, 2020).

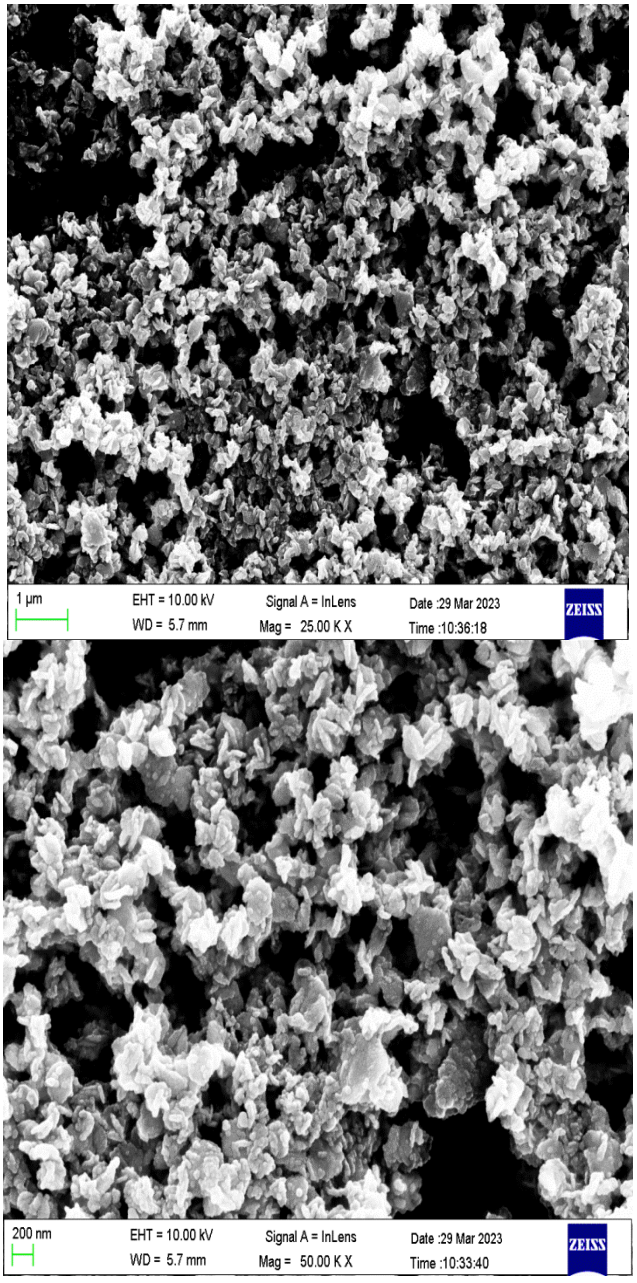

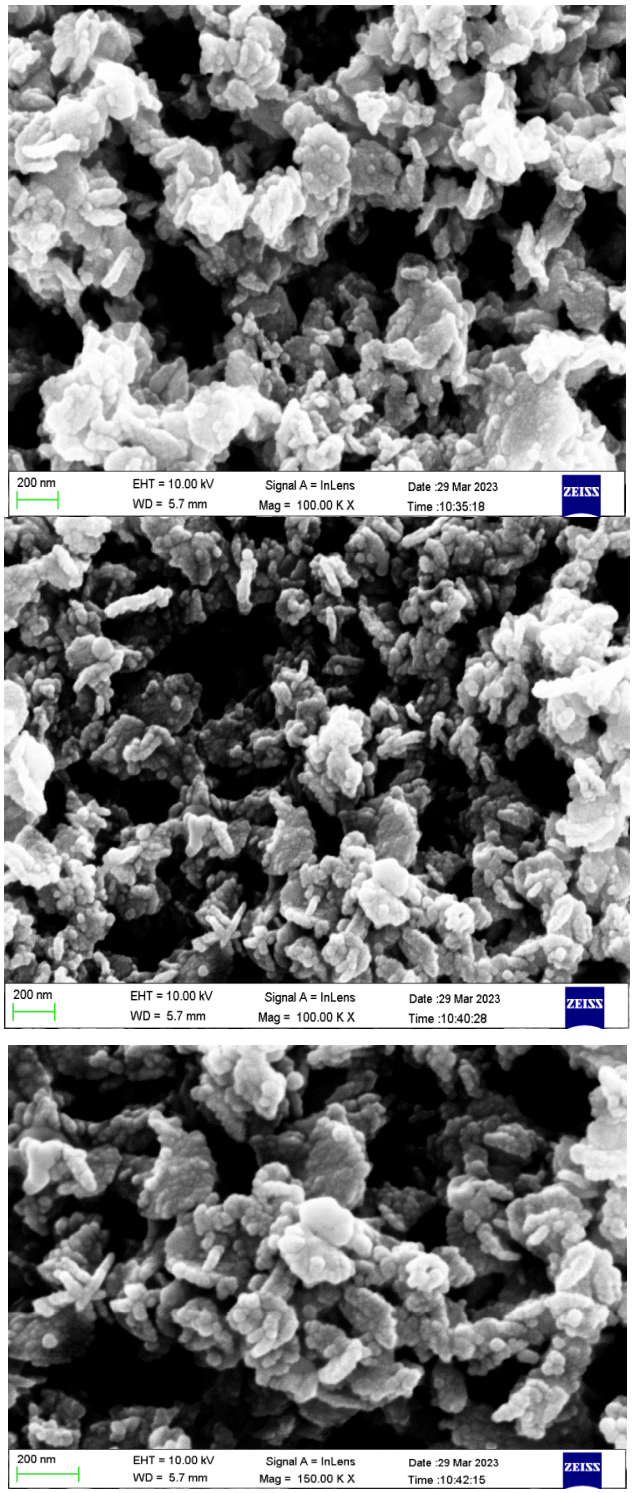

Fig. 4: (a) A lower magnification image (2500X) showing the chain-like arrangement of bigger silver nanoparticles. **(b)** Greater magnification (5000X) of silver nanoparticles of a bigger size **(c)** A silver nanoparticle image at a higher magnification (10000X) showing the existence of smaller silver nanoparticles. **(d)** A 15000X magnification of a silver nanoparticle image showing the presence of smaller silver nanoparticles

Figure 4 displays the SEM image of the created silver nanoparticles. The synthetic silver nanoparticles are spherical in form and evenly disseminated without any agglomeration, as seen by the SEM images. The larger particles joined to each other synchronously and created a structure resembling a chain. The outer layer over the nanoparticles is seen in the higher magnification image; this may be because the phytochemicals and alkaloids in banana stem extract surround and cap the nanoparticles. The aggregation of the nanoparticles has also been reduced as a result of the capping agent's presence. The SEM image reveals a wide size distribution of nanoparticles, including very small (5 nm) and large (120 nm) particles (Zhang, et al., 2016).

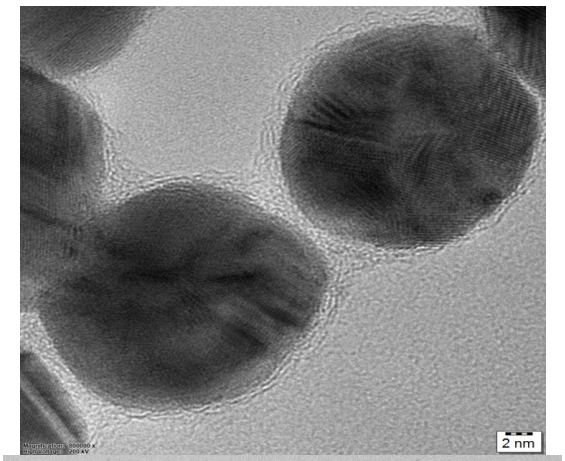

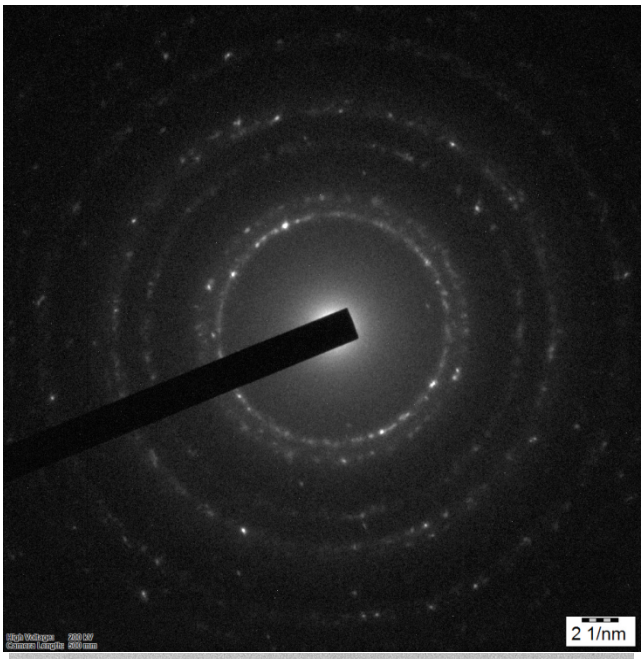

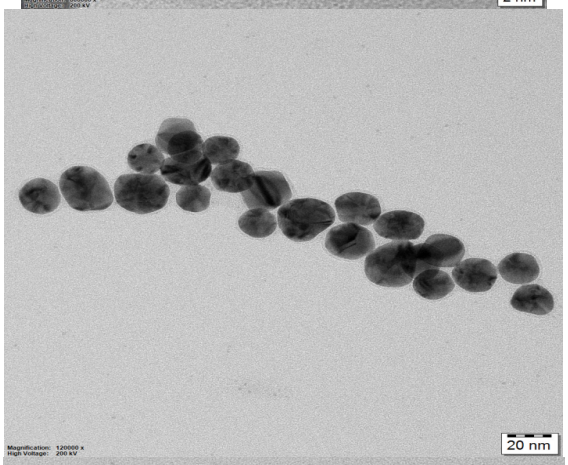

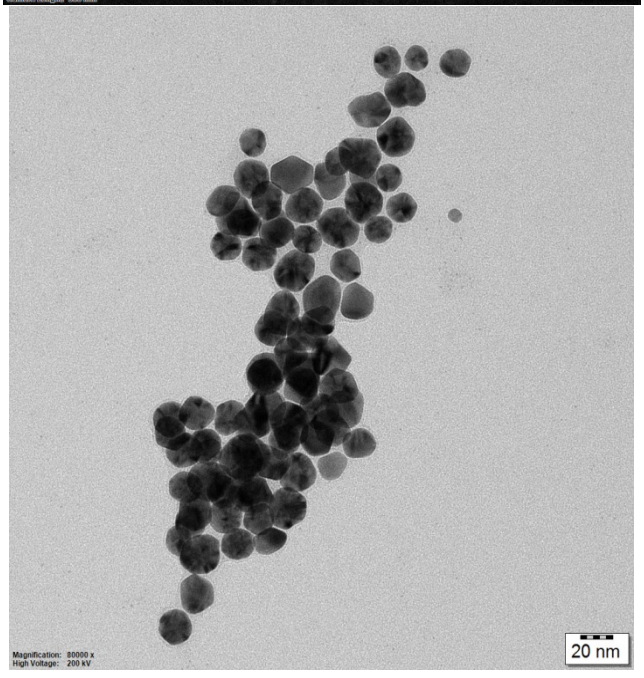

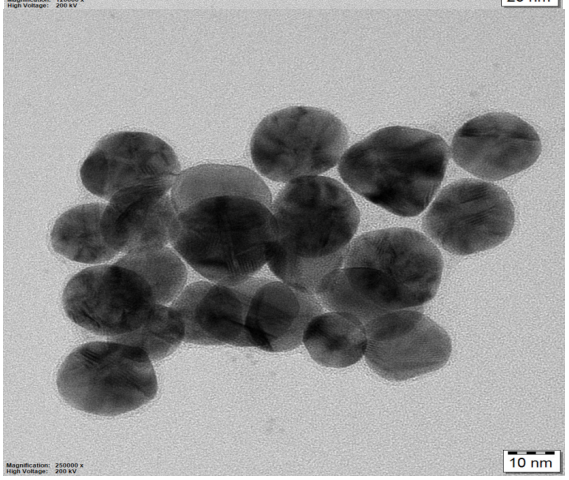

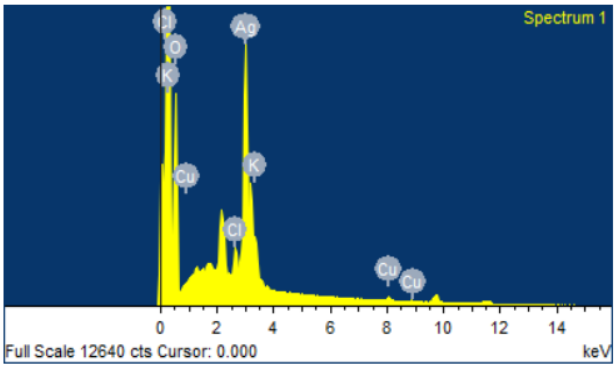

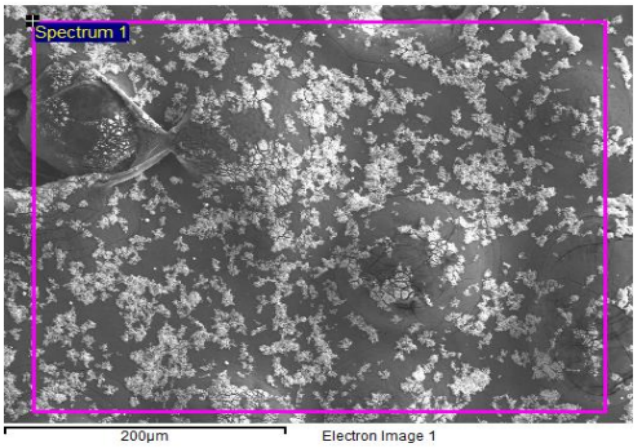

Fig. 5: (a) A TEM image showing the size of nanoparticles and a histogram of particle sizes **(b)** The silver nanoparticles' interplaner spacing **(c)** A lower magnification TEM picture showing the spread of nanoparticles **(d)** Silver nanoparticle EDAX spectra.

Using TEM, it was possible to determine the precise size, shape, and composition of the final particles (Figure 5). Ag nanoparticles were suspended in a diluted solution and cast onto copper grids. The grids were then allowed to dry for 48 hours before a TEM picture was taken (Ali et al., 2023). According to the TEM images, the silver nanoparticles were between 15 and 20 nm in size. The majority of the particles were spheres. The size determined by the TEM study was less than the size determined by the DLS analysis. The pure face-centered cubic (fcc) silver structural plane and the atomic plane distance were both found to be 1.4. The presence of silver nanoparticles is also supported by the peak at 3keV in the EDAX spectra (Wang, et al., 2021).

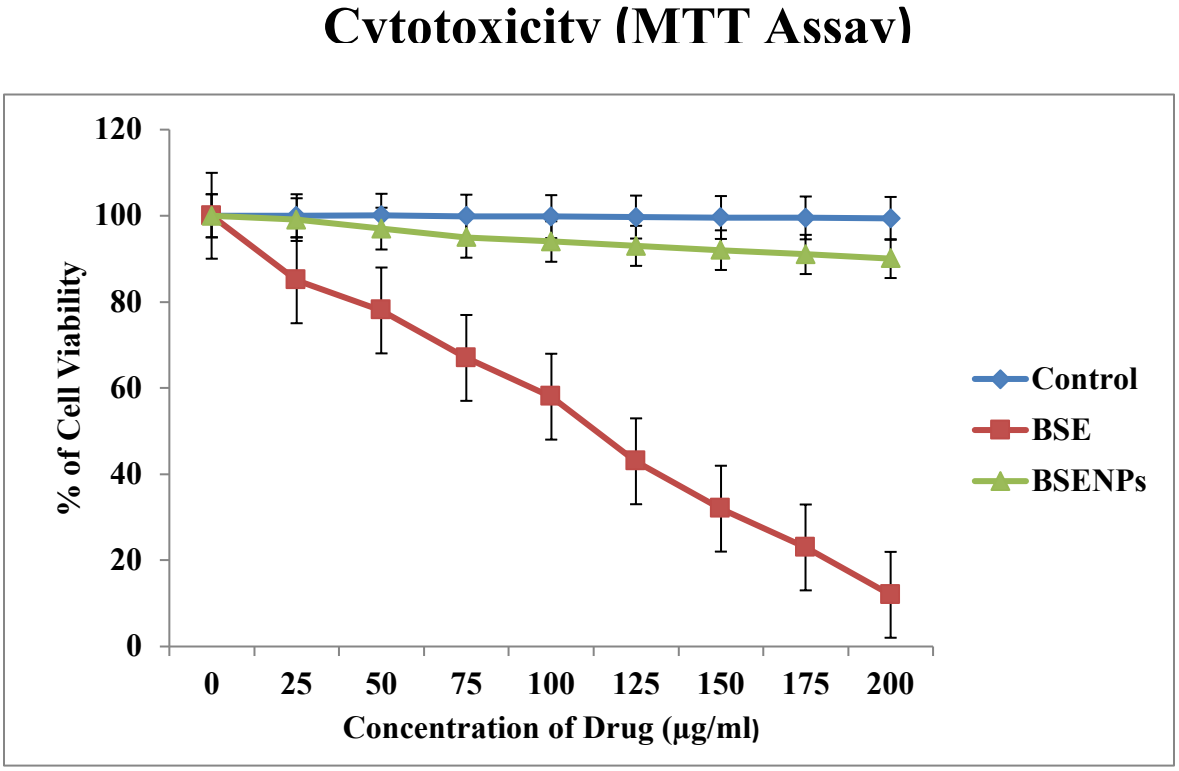

Fig. 6: Free Banana stem extract (BSE) and Banana stem extract-loaded nanoparticles (BSENPs) cytotoxicity is dose-dependent

3.3. Cell viability in response to banana stem extract-loaded nanoparticles (BSENPs)

Figure 6 illustrates the cytotoxic effects of various concentrations of free BSE and BSENPs (25, 50, 75, 100, 125, 150, 175 & 200 mg/ml) on HeLa cells. Free BSE did not affect cell viability, which suggests that BSE is not hazardous to HeLa cells at any of the studied concentrations (Moradhaseli, et al., 2013). At high concentrations (25, 50, 75, 100, 125, 150, 175 & 200 mg/ml), BSENPs showed considerable cytotoxicity. Only 14% of the cells were viable after being treated with 150 mg/ml of BSENPs. Therefore, the following concentrations (25, 50, 75, 100, 125, 150, 175 & 200 mg/ml) were utilised for additional anticancer studies (Lichota, et al., 2018).

3.4. Effect of banana stem extract-loaded nanoparticles (BSENPs) on morphological alterations associated with apoptosis

Figure 6 depicts the morphological changes that occur during apoptosis in various treatment groups. In contrast to control cells, which had equally dispersed green, fluorescent chromatin, BSENPs-treated cells had condensed or

fragmented chromatin, a sign of apoptosis (Elmore, 2007). The quantitative outcome of apoptosis in the various treatment groups is shown in Figure 6. These findings suggest that apoptosis may be the mode of cell death, together with membrane potential changes brought on by the BSENPs therapy (George, et al., 2022).

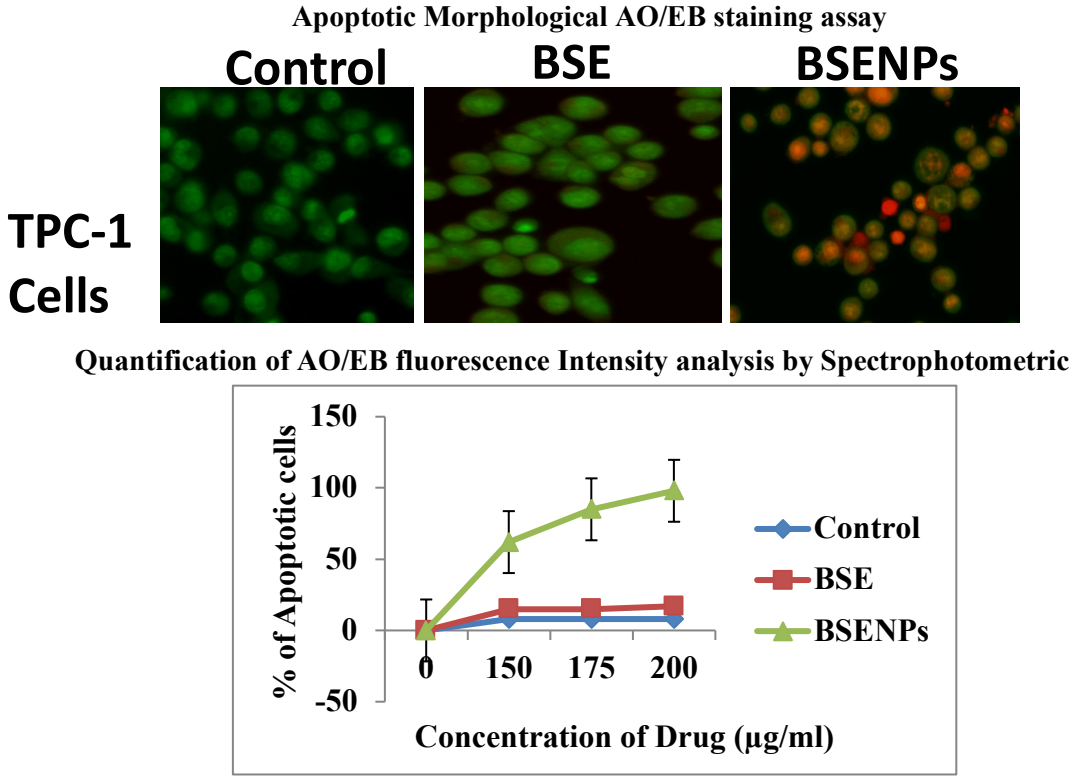

Fig. 7: (a) Dual-stained fluorescence microscopic pictures of apoptotic morphology. Late apoptotic, orange-colored cells are represented by the arrow mark **(a),** along with the percentage of apoptosis **(b).** The results of a one-way analysis of variance (ANOVA) followed by Duncan's multiple range test (DMRT) are shown as the mean SD of six experiments in each group. Values without the same superscript show a significant difference (P 0.05).

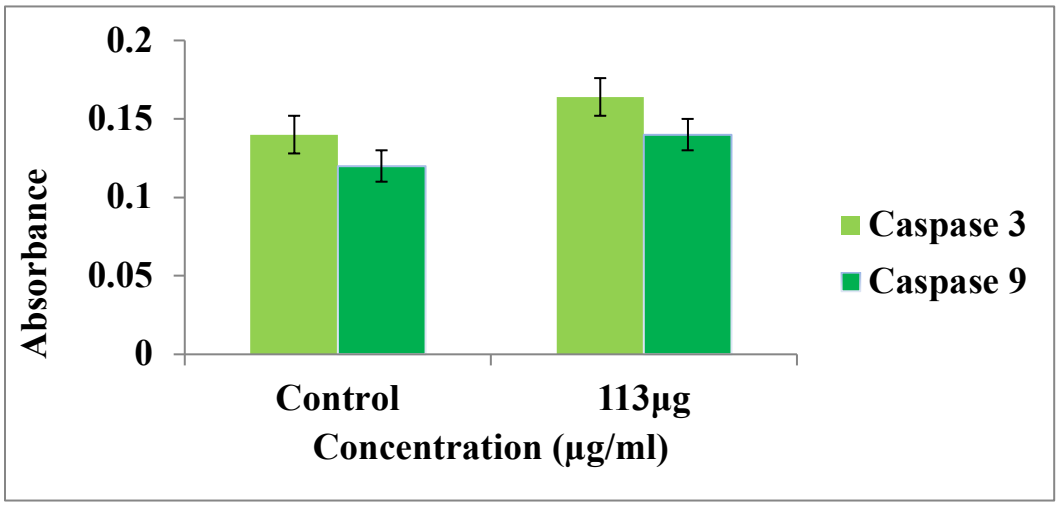

Fig. 8: (a) ELIZA methodologies study of the apoptotic marker proteins caspase 3 and caspase 9. The results of a one-way analysis of variance (ANOVA) followed by Duncan's multiple range test (DMRT) are shown as the mean SD of six experiments in each group. Significant differences between values without the common superscripts (P 0.05).

Figure 8(a) displays the variations in apoptotic marker protein expression across several treatment groups. Compared to control cells, which had evenly dispersed apoptotic protein, cells treated with BSENPs had higher expresses. The quantitative results of apoptosis in the various treatment groups are shown in Figure 8. These findings suggest that apoptosis may be the mode of cell death, along with mitochondrial change in the BSENPs treatment (Wu et al., 2016).

4 Conclusion

The current study focuses on one of the simple green synthesis methods for making silver nanoparticles utilising extract from banana stems. Different techniques were used to characterise the synthesised nanoparticles. The creation of silver nanoparticles was principally confirmed by the distinctive SPR peak at 420 nm in UV-Vis spectra. The DLS analysis verified the nanoparticles' hydrodynamic size and their prolonged stability in water for a month. SEM pictures revealed that bigger silver nanoparticles create a chain-like orientation, whereas smaller nanoparticles are often uniformly distributed. The TEM and EDAX investigation demonstrated that the majority of the nanoparticles were spherical in shape and corroborated the production and actual size of the silver nanoparticles. The silver nanoparticles' FCC crystal structure was likewise revealed by the XRD research, and the computed crystalline size was also within acceptable limits. When compared to conventional antibacterial drugs for both gramme positive and gramme negative bacteria, the biosynthesized silver nanoparticles also demonstrated good antibacterial efficacy. When compared to Diclofenac sodium, the silver nanoparticles with banana stem extract caps also showed greater in-vitro anti-cancer & apoptotic effects. This exploratory investigation may aid in the future development of anti-cancer and apoptotic impact drugs. Future aspects of this work will assess the silver nanoparticles' in-vivo and in-vitro toxicity levels in order to identify whether or not they may be used to treat humans.

References:

[1] Bayda S, Adeel M, Tuccinardi T, Cordani M, Rizzolio F. The History of Nanoscience and Nanotechnology: From Chemical-Physical Applications to Nanomedicine. Molecules. 2019 Dec 27;25(1):112. doi: 10.3390/molecules25010112. PMID: 31892180; PMCID: PMC6982820

[2] Murthy SK. Nanoparticles in modern medicine: state of the art and future challenges. Int J Nanomedicine. 2007;2(2):129-41. PMID: 17722542; PMCID: PMC2673971.

[3] Jeevanandam J, Barhoum A, Chan YS, Dufresne A, Danquah MK. Review on nanoparticles and nanostructured materials: history, sources, toxicity and regulations. Beilstein J Nanotechnol. 2018 Apr 3;9:1050-1074. doi: 10.3762/bjnano.9.98. PMID: 29719757; PMCID: PMC5905289

[4] Yaqoob AA, Ahmad H, Parveen T, Ahmad A, Oves M, Ismail IMI, Qari HA, Umar K, Mohamad Ibrahim MN. Recent Advances in Metal Decorated Nanomaterials and Their Various Biological Applications: A Review. Front Chem. 2020 May 19;8:341. doi: 10.3389/fchem.2020.00341. PMID: 32509720; PMCID: PMC7248377.

[5] Xu L, Wang YY, Huang J, Chen CY, Wang ZX, Xie H. Silver nanoparticles: Synthesis, medical applications and biosafety. Theranostics. 2020 Jul 11;10(20):8996-9031. doi: 10.7150/thno.45413. PMID: 32802176; PMCID: PMC7415816.

[6] Beyene HD, Werkneh AA, Bezabh HK, Ambaye TG. Synthesis paradigm and applications of silver nanoparticles (AgNPs), a review. Sustainable Materials and Technologies. 2017 Sep;13:18–23. doi: 10.1016/j.susmat.2017.08.001. Epub 2017 Aug 24. PMCID: PMC7148648.

[7] Bhardwaj B, Singh P, Kumar A, Kumar S, Budhwar V. Eco-Friendly Greener Synthesis of Nanoparticles. Adv Pharm Bull. 2020 Sep;10(4):566-576. doi: 10.34172/apb.2020.067. Epub 2020 Aug 9. PMID: 33072534; PMCID: PMC7539319.

[8] Iravani S, Korbekandi H, Mirmohammadi SV, Zolfaghari B. Synthesis of silver nanoparticles: chemical, physical and biological methods. Res Pharm Sci. 2014 Nov-Dec;9(6):385-406. PMID: 26339255; PMCID: PMC4326978.

[9] Naganthran A, Verasoundarapandian G, Khalid FE, Masarudin MJ, Zulkharnain A, Nawawi NM, Karim M, Che Abdullah CA, Ahmad SA. Synthesis, Characterization and Biomedical Application of Silver Nanoparticles. Materials (Basel). 2022 Jan 6;15(2):427. doi: 10.3390/ma15020427. PMID: 35057145; PMCID: PMC8779869.

[10] Hemeg HA. Nanomaterials for alternative antibacterial therapy. Int J Nanomedicine. 2017 Nov 10;12:8211-8225. doi: 10.2147/IJN.S132163. PMID: 29184409; PMCID: PMC5689025.

[11] Bhattacharyya SS, Das J, Das S, Samadder A, Das D, De A, Paul S, Khuda-Bukhsh AR. Rapid green synthesis of silver nanoparticles from silver nitrate by a homeopathic mother tincture Phytolacca Decandra. Zhong Xi Yi Jie He Xue Bao. 2012 May;10(5):546-54. doi: 10.3736/jcim20120510. PMID: 22587977.

[12] Iravani S, Korbekandi H, Mirmohammadi SV, Zolfaghari B. Synthesis of silver nanoparticles: chemical, physical and biological methods. Res Pharm Sci. 2014 Nov-Dec;9(6):385-406. PMID: 26339255; PMCID: PMC4326978.

[13] Ahsan A, Farooq MA, Ahsan Bajwa A, Parveen A. Green Synthesis of Silver Nanoparticles Using Parthenium Hysterophorus: Optimization, Characterization and In Vitro Therapeutic Evaluation. Molecules. 2020 Jul 22;25(15):3324. doi: 10.3390/molecules25153324. PMID: 32707950; PMCID: PMC7435648.

[14] Stetefeld J, McKenna SA, Patel TR. Dynamic light scattering: a practical guide and applications in biomedical sciences. Biophys Rev. 2016 Dec;8(4):409-427. doi: 10.1007/s12551-016-0218-6. Epub 2016 Oct 6. PMID: 28510011; PMCID: PMC5425802

[15] Arokiyaraj S, Arasu MV, Vincent S, Prakash NU, Choi SH, Oh YK, Choi KC, Kim KH. Rapid green synthesis of silver nanoparticles from Chrysanthemum indicum L and its antibacterial and cytotoxic effects: an in vitro study. Int J Nanomedicine. 2014;9:379-88. doi: 10.2147/IJN.S53546. Epub 2014 Jan 7. PMID: 24426782; PMCID: PMC3890422.

[16] Jagtap RR, Garud A, Puranik SS, Rudrapal M, Ansari MA, Alomary MN, Alshamrani M, Salawi A, Almoshari Y, Khan J, Warude B. Biofabrication of Silver Nanoparticles (AgNPs) Using Embelin for Effective Therapeutic Management of Lung Cancer. Front Nutr. 2022 Aug 4;9:960674. doi: 10.3389/fnut.2022.960674. PMID: 35990347; PMCID: PMC9386231.

[17] Sharma VK, Yngard RA, Lin Y. Silver nanoparticles: green synthesis and their antimicrobial activities. Adv Colloid Interface Sci. 2009 Jan 30;145(1-2):83-96. doi: 10.1016/j.cis.2008.09.002. Epub 2008 Sep 17. PMID: 18945421.

[18] Buranaamnuay K. The MTT assay application to measure the viability of spermatozoa: A variety of the assay protocols. Open Vet J. 2021 Apr-Jun;11(2):251-269. doi: 10.5455/OVJ.2021.v11.i2.9. Epub 2021 May 8. PMID: 34307082; PMCID: PMC8288735.

[19] Sigmon J, Larcom LL. The effect of ethidium bromide on mobility of DNA fragments in agarose gel electrophoresis. Electrophoresis. 1996 Oct;17(10):1524-7. doi: 10.1002/elps.1150171003. PMID: 8957173.

[20] Sathishkumar M, Sneha K, Won SW, Cho CW, Kim S, Yun YS. Cinnamon zeylanicum bark extract and powder mediated green synthesis of nano-crystalline silver particles and its bactericidal activity. Colloids Surf B Biointerfaces. 2009 Oct 15;73(2):332-8. doi: 10.1016/j.colsurfb.2009.06.005. Epub 2009 Jun 10. PMID: 19576733.

[21] Salgame P, Varadhachary AS, Primiano LL, Fincke JE, Muller S, Monestier M. An ELISA for detection of apoptosis. Nucleic Acids Res. 1997 Feb 1;25(3):680-1. doi: 10.1093/nar/25.3.680. PMID: 9016614; PMCID: PMC146463.

[22] Soni P, Siddiqui AA, Dwivedi J, Soni V. Pharmacological properties of Datura stramonium L. as a potential medicinal tree: an overview. Asian Pac J Trop Biomed. 2012 Dec;2(12):1002-8. doi: 10.1016/S2221-1691(13)60014-3. PMID: 23593583; PMCID: PMC3621465.

[23] Zeng L, Zhang Q, Jiang C, Zheng Y, Zuo Y, Qin J, Liao Z, Deng H. Development of *Atropa belladonna* L. Plants with High-Yield Hyoscyamine and without Its Derivatives Using the CRISPR/Cas9 System. Int J Mol Sci. 2021 Feb 9;22(4):1731. doi: 10.3390/ijms22041731. PMID: 33572199; PMCID: PMC7915368.

[24] Iravani S, Korbekandi H, Mirmohammadi SV, Zolfaghari B. Synthesis of silver nanoparticles: chemical, physical and biological methods. Res Pharm Sci. 2014 Nov-Dec;9(6):385-406. PMID: 26339255; PMCID: PMC4326978.

[25] Erdogan O, Abbak M, Demirbolat GM, Birtekocak F, Aksel M, Pasa S, Cevik O. Green synthesis of silver nanoparticles via Cynara scolymus leaf extracts: The characterization, anticancer potential with photodynamic therapy in MCF7 cells. PLoS One. 2019 Jun 20;14(6):e0216496. doi: 10.1371/journal.pone.0216496. PMID: 31220110; PMCID: PMC6586393.

[26] Zhang XF, Liu ZG, Shen W, Gurunathan S. Silver Nanoparticles: Synthesis, Characterization, Properties, Applications, and Therapeutic Approaches. Int J Mol Sci. 2016 Sep 13;17(9):1534. doi: 10.3390/ijms17091534. PMID: 27649147; PMCID: PMC5037809.

[27] Ali IAM, Ahmed AB, Al-Ahmed HI. Green synthesis and characterization of silver nanoparticles for reducing the damage to sperm parameters in diabetic compared to metformin. Sci Rep. 2023 Feb 8;13(1):2256. doi: 10.1038/s41598-023-29412-3. Erratum in: Sci Rep. 2023 Apr 24;13(1):6659. PMID: 36755090; PMCID: PMC9908928.

[28] Wang M, Shen J, Thomas JC, Mu T, Liu W, Wang Y, Pan J, Wang Q, Liu K. Particle Size Measurement Using Dynamic Light Scattering at Ultra-Low Concentration Accounting for Particle Number Fluctuations. Materials (Basel). 2021 Sep 29;14(19):5683. doi: 10.3390/ma14195683. PMID: 34640079; PMCID: PMC8510349.

[29] Moradhaseli S, Zare Mirakabadi A, Sarzaeem A, Kamalzadeh M, Haji Hosseini R. Cytotoxicity of ICD-85 NPs on Human Cervical Carcinoma HeLa Cells through Caspase-8 Mediated Pathway. Iran J Pharm Res. 2013 Winter;12(1):155-63. PMID: 24250584; PMCID: PMC3813208.

[30] Lichota A, Gwozdzinski K. Anticancer Activity of Natural Compounds from Plant and Marine Environment. Int J Mol Sci. 2018 Nov 9;19(11):3533. doi: 10.3390/ijms19113533. PMID: 30423952; PMCID: PMC6275022.

[31] Elmore S. Apoptosis: a review of programmed cell death. Toxicol Pathol. 2007 Jun;35(4):495-516. doi: 10.1080/01926230701320337. PMID: 17562483; PMCID: PMC2117903.

[32] George BP, Rajendran NK, Houreld NN, Abrahamse H. *Rubus* Capped Zinc Oxide Nanoparticles Induce Apoptosis in MCF-7 Breast Cancer Cells. Molecules. 2022 Oct 13;27(20):6862. doi: 10.3390/molecules27206862. PMID: 36296460; PMCID: PMC9611499.

[33] Wu Y, Zhao D, Zhuang J, Zhang F, Xu C. Caspase-8 and Caspase-9 Functioned Differently at Different Stages of the Cyclic Stretch-Induced Apoptosis in Human Periodontal Ligament Cells. PLoS One. 2016 Dec 12;11(12):e0168268. doi: 10.1371/journal.pone.0168268. PMID: 27942018; PMCID: PMC5152893.